Taylor & Francis
Taylor & Francis Group

RESEARCH PAPER

OPEN ACCESS | Check for updates

# SIA-IgG confers poor prognosis and represents a novel therapeutic target in breast cancer

Man Zhang[a],*, Jinhua Zheng[b],*, Junying Guo[a],*, Qiujin Zhang[a], Juan Du[a], Xiangfeng Zhao[a], Zhihua Wang[a], and Qinyuan Liao [a]

[a]Department of Immunology, Guilin Medical University, Guilin, Guangxi province, China; [b]Department of Pathology, Guilin Medical University Affiliated Hospital, Guilin, Guangxi province, China
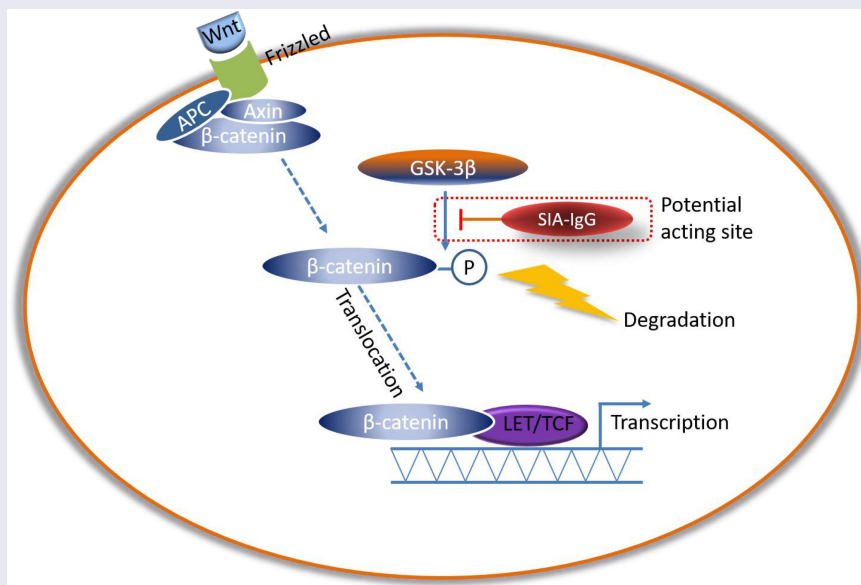
## ABSTRACT

The incidence rate of breast cancer is the highest in the world, and major problem in the clinical treatment is the therapy resistance of breast cancer stem cells (CSCs). Thus, new therapeutic approaches targeting breast CSCs are needed. Our previous study demonstrated cancer-derived sialylated IgG (SIA-IgG) is highly expressed in cancer cells with stem/progenitor features. Furthermore, a high frequency of SIA-IgG in breast cancer tissue predicted metastasis and correlated with poor prognosis factors, and depletion of IgG in breast cancer leads to lower malignancy of cancer cells, suggesting SIA-IgG could be a potential therapeutic target in breast cancer. In this study, we first investigated the relationship of SIA-IgG expression with the clinicopathological characteristics and clinical prognosis of breast carcinoma patients, and the data confirmed that the expression of SIA-IgG confers poor prognosis in breast cancer. Successively, by using a monoclonal antibody specifically against SIA-IgG, we targeted SIA-IgG on the surface of MDA-MB-231 cells and detected their functional changes, and the results suggested SIA-IgG to be a promising antibody therapeutic target in breast cancer. In addition, we explored the mechanism of action at the molecular level of SIA-IgG on breast cancer cell, the findings suggest that SIA-IgG promotes proliferation, metastasis, and invasion of breast cancer cells through the Wnt/β-catenin signaling pathway. Developing therapeutic antibody needs effective therapeutic target, and the antibody should better be a monoclonal antibody with high affinity and high specificity. This study provides a potential prognostic marker and a novel therapeutic target for breast cancer.

## Highlights

- SIA-IgG confers poor prognosis in breast cancer.
- The monoclonal antibody RP215 is a potential therapeutic antibody in breast cancer.
- SIA-IgG may affect the biological function of breast cancer cells by regulating *Wnt*/β-catenin signaling pathway.

## Introduction

The incidence of breast cancer has risen dramatically in recent decades, and breast cancer is one of the leading causes of cancer mortality worldwide [1–3]. Patients with a favorable subtype can expect an overall survival (OS) above 95% and a local control rat (LCR) of almost 100% over 5 years. On the other hand the outcome of patients with HER2 and Triple negative subtypes remains poor, thus necessitating more intensified research and care [4]. Metastasis accounts for the majority of breast carcinoma deaths, however, the pathogenetic mechanisms have not been fully elucidated, and the molecular mechanisms that orchestrate cancer metastasis remain poorly understood until now [5,6]. In studies of this aspect, accumulating data have shown that cancer stem cells (CSCs) play important roles in breast cancer metastasis, recurrence, drug resistance and worse prognosis, and traditional breast cancer therapies are effective in killing only the majority of tumor cells while leaving CSCs alive, driving drug resistance and cancer relapse [7–9]. Novel therapies targeting breast CSCs may remove the barrier for achieving curability. On the other hand, one molecular hallmark of cancer is aberrant glycosylation, and malignant transformation is accompanied by changes in both N- and O-glycosylation of proteins [10,11]. In breast carcinomas, the relationship between glycosylation and cancer metastasis has been an important scientific topic in recent decades. O-linked glycans are frequently truncated, often as a result of premature sialylation [12–15]. Glycotherapy is one of the potential therapeutic strategies to target aberrant glycosylation, promoting abnormal cellular activities and carcinogenesis [16].

SIA-IgG, a non-B cell-derived immunoglobulin (Ig) and a potential breast CSC marker with aberrant glycosylation, is also a potential cancer therapeutic target. Increasing evidence has proven that immunoglobins (Igs) can also be produced and derived by many other kinds of cells in addition to B cells, and the rearrangements, transcripts and proteins of IgA, IgM, IgG and IgE are widely expressed in multiple non-B cell types, especially in cancer cells [17–30]. Currently, most cancer-Ig studies focus on IgG, which is considered to be associated with tumor progression, metastasis, and poor prognosis in kinds of human epithelia cancers and soft tissue tumors, such as breast cancer, pancreatic cancer and sarcomas [31–35]. By utilizing the monoclonal antibody RP215, which is specific to an abnormal sialic acid-modified epitope within the CH1 domain of non-B cell-derived IgG (non B-IgG) [36–39], researchers could study the expression, localization, and function of sialic acid IgG (SIA-IgG), and interference with B cell-derived IgG (B-IgG) contributions could be excluded. We first discovered that this type of SIA-IgG was found in multiple classes of cells with epithelial origin, especially in epithelial tumor cells with high frequency [40]. Interestingly, we found that SIA-IgG was highly expressed in breast cancer stem/progenitor-like cells [40]. Further research on the role of SIA-IgG in epithelial cancer was performed, and other researchers and us have demonstrated that the expression of SIA-IgG was correlated with high malignancy of cancer cells and often appears to be associated with poor prognosis of patients [40–44]. Lung Squamous Cell Carcinoma (LSCC) patients with high SIA-IgG expressing level had significantly shorter disease free survival (DFS) (N = 68, $P$ = 0.0073), and multivariate Cox regression analysis demonstrated that SIA-IgG expressing level is strongly associated with patients' survival (HR = 3.744, $P$ = 0.013) [39].In 140 lung adenocarcinomas (ADC) cases, the expressing level of SIA-IgG is significantly correlated with local invasion ($P$ < 0.05) and tumor differentiation ($P$ < 0.05), and Cox multivariate analysis also showed SIA-IgG (HR = 5.102, $P$ < 0.0001) is an independent risk factor of poor prognostic for ADC patients [41]. Another

research in 381 patients of Pancreatic Ductal Adenocarcinoma (PDA), SIA-IgG expression was identified as an independent prognostic factor associated with both DFS (HR = 2.359, P < 0.001)and Overall survival (OS) (HR = 2.490, P < 0.001)by the multivariate Cox regression analysis DFS:HR = 2.359, P < 0.001; OS: 2.490, P < 0.001) [41]. There are also researches showing that SIA-IgG promotes the development of prostate cancer and bladder cancer *in vitro* [42,45] and in our previous study of breast cancer, increasing SIA-IgG expressing level in beast cancer predicted metastasis and correlate with poor prognosis factors. In our previous work, the results also indicated a strong positive correlation and colocalization between SIA-IgG^{high} breast cancer cells and CD44^{+}/CD24^{low/−} breast CSCs [40], suggesting that SIA-IgG might be a potential treatment target for CSCs in breast cancer. In addition, further studies are needed to confirm this.

In this research, after following clinical patients and collecting tumor specimens, we evaluated the relationship between the expression of SIA-IgG and clinicopathological characteristics and poor prognosis in 75 cases of breast cancer with overall survival (OS) by immunohistochemistry. The results suggest that SIA-IgG could serve as a useful indicator for the poor prognosis of breast cancer and a possible clinical treatment target.

In our previous study, we knockdown the expression of SIA-IgG in breast cancer cell line MDA-MB-231, a Triple negative breast cancer cell line, and the leads to reduced adhesion, invasion and self-renewal and increased apoptosis of cancer cells, indicate that targeting SIA-IgG is feasible in the treatment of breast cancer, especially for Triple negative breast cancer [40]. As the safety of gene therapy in cancer remains unclear, and the localization of SIA-IgG is primarily localized on the cell surface, we prefer to antibody treatment by utilize the monoclonal antibody RP215 which specific to SIA-IgG.

In Lee group's research, RP215 treatments can induce apoptosis in various cancer cells, suggesting that this monoclonal antibody could block the function of SIA-IgG [46,47]. In this study, using the antibody RP215, we blocked the specific glycosylation site of SIA-IgG on the surface and secreted it by MDA-MB-231 cells and explored the changes in their biological characteristics, such as proliferation, migration, invasion and apoptosis. The data have shown that SIA-IgG could be a therapeutic target and has the potential for clinical application.

This work also explored the signaling mechanisms of the activities of SIA-IgG on breast cancer cells. In the preceding study, after the expression of IgG was knocked down in MDA-MB-231 cells, the total RNA was extracted and RNA sequencing was performed. The analyze data indicated SIA-IgG regulate biological characteristics of MDA-MB -231 cells may through *Wnt* signaling pathway (data not shown), other researcher also demonstrated *Wnt*/β-catenin pathway plays an important role in the proliferation and epithelial-mesenchymal transition (EMT) phenotype in breast cancer cells [48,49]. At the present study, we confirm this finding that SIA-IgG may regulate *Wnt*/β-catenin pathway via mediate GSK3β phosphorylation and inhibition. In conclusion, based on the prophase research, this study reveals a novel SIA-IgG/GSK3β mediated *Wnt*/β-catenin pathway that promotes breast cancer prognosis, and confirmed SIA-IgG as a novel indicator for poor outcome and a therapeutic target in breast cancer.

## Material and methods

### Patient samples

Formalin-fixed, paraffin-embedded samples of breast cancer were obtained from 75 patients from the Affiliated Hospital of Guilin Medical University (Guilin, Guangxi, China) and the First Affiliated Hospital of Guangxi Medical University (Nanning, Guangxi, China). In all, 66 of the samples were invasive ductal carcinoma, and 9 of the samples were invasive lobular carcinoma. The histological classification and grading of tumor specimens were based on the WHO classification. The tumor/node/metastasis (TNM) stage was determined according to the guidelines of the American Joint Committee on Cancer (AJCC). Clinicopathological data were obtained from a review of hospital medical records. All 75 breast cancer samples were female patients aged between 27 and 80 (45.5 ± 9.3) years. In histopathological

grading, 18.7% of the samples (n = 14) were well differentiated (grade I), 65.3% of the samples (n = 49) were moderately differentiated (grade II) and 16.0% (n = 12) were poorly differentiated (grade III). A total of 57.3% of patients (n = 43) developed lymph node metastasis. By TNM staging standards, 1 (1.3%) was in stage I, 29 (38.7%) in stage IIA, 32 (42.7%) in stage IIB, 12 (16%) in stage IIIA and 1 (1.3%) in stage IIIB. All patients were followed-up until August 2018. Ethical approval of the study was granted by the Ethics Committee of the Guilin Medical College, and informed consent was received from all participants prior to commencement of the study.

### Cell line and culture condition

The breast carcinoma cell-line MDA-MB-231, MCF-7 and the human breast epithelial cells MCF 10A was purchased from the American Type Culture Collection (ATCC). MDA-MB-231 cells maintained in RPMI 1640 medium with 10% fetal bovine serum, 100 U/ml penicillin, and 100 mg/ml streptomycin in a humidified 37°C incubator. MCF-7 cells were maintained in DMEM supplemented with 10% FBS. MCF-10A cells were cultured in a complete growth medium (CM-0525, Procell Life Science & Technology Company, Wuhan, China).

### Immunohistochemistry

Immunohistochemistry steps were performed by standard protocols. Antigen retrieval was conducted by immersing slides in Tris-EDTA buffer (pH 9.0) at 120°C for 3 min, and primary mAb RP215 (3.99 mg/ml) was provided by Xiaoyan Qiu of Peking University (the cell line of monoclonal antibody RP215 was generated by Gorgey Lee of the University of British Columbia in Vancouver, Canada), and the dilution was 1:3000. Secondary antibodies were from Jackson Immuno Research and Invitrogen, antigen was visualized with substrate chromogen (Dako liquid DAB chromogen; Dako), staining was performed according to the instructions. The expression of SIA-IgG was qualified by a four-

tier intensity score (0, none; 1, weak; 2, moderate; 3, strong) and the percentage (0–100%) of positive cells. The final staining score was obtained by multiplying the intensity and percentage of positive cells (range 0–300) according to the percentage of positive cells present among all tumor cells. A score ≥150 was defined as high SIA-IgG expression, while scores <150 were defined as low SIA-IgG expression.

### Colony formation assay

Cell viability was detected using a colony formation assay. Cells were seeded into the wells of 6-well plates (200 cells per well) for 6 hours, followed by treatment with blocking antibody to the cell culture medium after the cells adhered. The culture medium was renewed every 2 days. After 8 days, the cells were stained with 0.1% crystal violet to assess colony formation. Colonies containing >40 cells were counted [50]. This study was done in triplicate.

### Cell counting Kit-8 (CCK-8) assay

The proliferation ability of cells was determined by a CCK-8 colorimetric growth assay. Cells were cultured in 96-well plates ($2 \times 10^3$ cells per well) in complete medium for 6 hours, followed by treatment with blocking antibody to the cell culture medium after the cells adhered. Each day, the culture medium was renewed, and cell growth was determined by adding 10 μl CCK8 solution in 100 μl RPMI 1640 with 10% FBS for 2 h at 37°C. Then, the absorbance was measured with a 450-nmfilter. This study was done in five duplicates [51].

### In vitro wound healing assay

Cellular migration was evaluated by wound healing assay. MDA-MB-231 cells ($2 \times 10^5$) were grown to confluence on 12-well plates in RPMI 1640 (1 ml per well) with 1% FBS. After 12 h, a scratch was introduced with a sterile 200 μl pipette tip, washed twice with PBS, and then treated with blocking antibody to the cell culture medium.

Cells were further cultured in RPMI 1640 with 1% FBS, and then areas refilled by migrating MDA-MB-231 cells were documented. Cell migration was observed under a phase-contrast inverted microscope (Zeiss; 5× magnification), and images of four selected areas were captured and analyzed every 24 h until the wound healed [52]. This study was done in triplicate.

### Transwell migration and Matrigel invasion assays

The migration ability of breast cells was detected using a Transwell assay. The assays were performed using polycarbonate membrane transwell inserts with pore size of 8.0 μm (Corning, USA and Jet Biofil, China) was used for the migration assay. For the invasion assay, a Corning® Matrigel® Invasion Chamber (Corning, USA) was used. Cells were seeded into the upper chamber at a density of $3 \times 10^4$ cells in 200 μl serum-free medium, and the bottom chamber was filled with 500 μl medium containing 10% FBS. After incubation for 6 h at 37°C, blocking antibody was added to the cell culture medium as the cells adhered, and the cells were incubated for 24 h or 48 h at 37°C in a humidified 5% CO2 atmosphere. Cells in the top chamber were removed by a cotton-tipped swab, and the migrated cells were stained with crystal violet. They were then visualized under a phase-contrast microscope and photographed. These studies were done in triplicate. The number of migrated/invaded cells was counted in six random fields under an inverted microscope (Olympus BX53; 10× magnification) [53,54].

### Apoptosis assay based on Annexin V-FITC/ propidium iodide (PI) flow cytometry

Apoptosis was determined by using an Annexin V-FITC Apoptosis Detection kit (cat. no. 556547; BD Biosciences). Flow cytometry can distinguish early apoptotic cells, late apoptotic cells and normal cells. The experimental steps were performed according to the manufacturer's protocol, and data acquisition and analysis were performed using flow cytometry (FACScan; BD Biosciences) and FlowJo software (version 10.0; FlowJo LLC). The results for early and late apoptosis were combined as the total amount of apoptosis.

### siRNA transfection

Inhibition of IgG expression was achieved through siRNA transfection by electroporation on a Gene Pulser XCell (BioRad). The siRNAs against Ig gamma chain constant region (siIgG1 and siIgG2) and the control RNA (NC) (siIgG1: 5′-GGUGGACAAGACAGUUGAG-3′, siIgG2: 5′-AGUGCAAGGUCUCCAACAA-3′, NC: 5′-UUCUCCGAACGUGUCACGU-3′) purchased from Shanghai GenePharma Corporation, China. Cell density was adjusted to $2 \times 10^6$/350 μl. The knockdown efficiency of IgG was checked by Western blot.

### Western blotting

Whole-cell extracts were prepared in cell lysis buffer (10 mM Tris-HCl, 1% Triton-X 100, 1% sodium deoxycholate, 0.1% sodium dodecyl sulfate [SDS], 0.15 M NaCl, with protease inhibitor cocktail from Roche Applied Science [Indianapolis, IN]). Western blot was performed using standard protocols.

### Xenograft mouse model

Five-week-old healthy female BALB/C nude mice were purchased from Hunan Silaikejingda Laboratories (Hunan, China) and used in a xenograft mouse model. The mice were allowed to acclimate for 1 week after arrival. $1 \times 10^6$ MDA-MB-231 cells were injected (100 μl per site) injected subcutaneously into the axilla of mice, and when tumors were ready (21 d), three groups of nude mice were subjected to peritumoral injection with 30 μl of monoclonal RP215 (5 μg/tumor), control IgG antibody (mouse IgG, #400402, BioLegend, 5 μg/tumor), and saline every 5 days. Tumor size was monitored on the second day, and the tumor volumes were calculated using the following formula: tumor
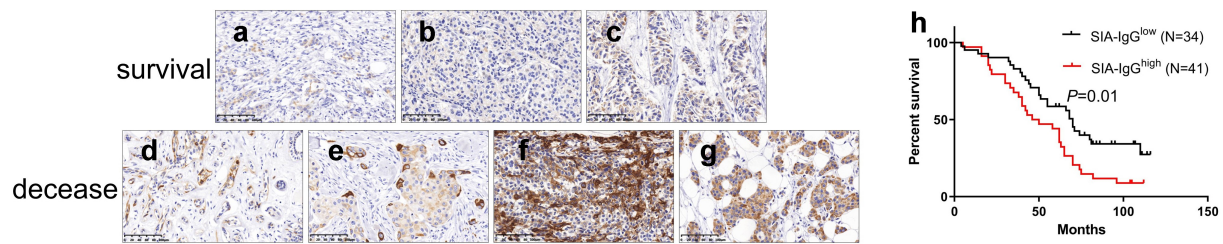
**Figure 1.** **The expression of SIA-IgG is correlated with clinical prognosis in breast cancer**. Immunohistochemistry staining for SIA-IgG in breast cancer tissues. For example, infiltrating ductal carcinoma showed weak SIA-IgG-positive staining in the tissues of surviving patients (**a, b**, and **c**) and strong SIA-IgG-positive staining in the tissues of deceased patients (**d, e, f**, and **g**) with invasive breast cancer. The clinical characteristics of the tissues are as follows: (a) well differentiated (grade I), without lymph node metastasis, TNM stage IIA. (b) moderately differentiated (grade I), without lymph node metastasis, TNM stage IIB. (c) moderately differentiated (grade II), with lymph node metastasis (TNM-N1), TNM stage IIIA. (d) moderately differentiated (grade II), with lymph node metastasis (TNM-N2), TNM stage IIA. (e) moderately differentiated (grade II), without lymph node metastasis, TNM stage IIB. (f) moderately differentiated (grade II), with lymph node metastasis (TNM-N1), TNM stage IIIA. (g) moderately differentiated (grade II), with lymph node metastasis (TNM-N1), TNM stage IIIB. (h) Kaplan–Meier survival for SIA-IgG high expression and low expression groups. Patients in the SIA-IgG high expression group (SIA-IgG$^{high,}$ staining score ≥ 150) had a significantly poorer prognosis than those in the SIA-IgG low expression (SIA-IgG$^{low}$, staining score < 150) group ($P$ = 0.01).

volume = $0.52 \times \text{width}^2 \times \text{length}$. Then, after 2 weeks, the mice were sacrificed. Animal ethical approval of the study was granted by the Animal Ethics Committee of Guilin Medical College. All animal experiments were complied with the ARRIVE guidelines, and all procedures followed the National Institutes of Health Guide for the Care and Use of Laboratory Animals.

## Statistical analysis

The relationship between SIA-IgG expression and clinicopathological features (age, tumor size, pathological grade, local invasion, lymph node metastasis, TNM stage and discovery time) was assessed using the chi-square test and Mann–Whitney test. Date of breast cancer diagnosis was defined as time zero for the calculation of survival rates. Survival was defined as time from diagnosis to death, or to last follow-up if death had not occurred. Patients who died were not censored. Surviving patients were censored [55]. Overall survival (OS) was calculated by Kaplan–Meier analysis and compared using the log-rank test. A Cox proportional hazards model was used to identify the prognostic effect of SIA-IgG on survival. All the clinical data were analyzed with SPSS 19 software, and all data based on the breast cancer cell-line MDA-MB-231 were analyzed with GraphPad Prism software and presented as the mean ±

standard error of the mean. Statistical significance was determined by the two-tailed unpaired t test with a significance level of $P$ value < 0.05.

## Results

### High SIA-IgG expression is associated with poor prognosis of breast cancer patients

In our previous study, data showed that the expression of SIA-IgG was significantly higher in metastatic samples than in situ breast cancer and correlated with poor prognosis factors [40]. In this study, we first analyzed the relationship between SIA-IgG expression and the clinicopathological features of tissues from 75 breast cancer patients. Both the positive rate and staining score of SIA-IgG were significantly correlated with metastasis ($P$ = 0.035, χ2; $P$ = 0.036, Mann–Whitney) and TNM stage ($P$ = 0.027, χ2; $P$ = 0.012, Mann–Whitney), indicating that SIA-IgG expression was significantly higher in breast cancer cases with greater migration capacity. No significant correlations between SIA-IgG positivity and age, tumor size, pathological grade, local invasion (TNM-T) or discovery time were observed (Figure 1(a–g)); (Table 1).

To further confirm that the expression of SIA-IgG is associated with poor prognosis of breast carcinoma patients, the correlation between SIA-

**Table 1.** Association between SIA-IgG expression and clinicopatholioical characteristics.

| Clinical characteristics | cases $n$ | Positive cases $n$(%) | $P$-value$^a$($\chi^2$) | SIA-IgG staining score mean (SD) | $P$-value$^b$ (Mann -Whitney) |
|---|---|---|---|---|---|
| Ages (years) | | | 0.302 | | 0.305 |
| <50 | 53 | 22 (41.51) | | 125.09 (69.85) | |
| ≥50 | 22 | 12 (54.55) | | 139.09 (83.38) | |
| Tumor size (cm) | | | 0.072 | | 0.074 |
| <5 | 35 | 12(34.29) | | 115.71 (67.44) | |
| ≥5 | 40 | 22 (55.00) | | 141.00(77.82) | |
| Pathological grade | | | 0.192 | | 0.108 |
| I-II | 63 | 26(41.27) | | 121.27(72.19) | |
| III-IV | 12 | 8(66.67) | | 170.83 (70.64) | |
| TNM-T | | | 0.117 | | 0.120 |
| T1-T2 | 49 | 19 (38.78) | | 115.10 (65.71) | |
| T3-T4 | 26 | 15 (57.69) | | 155.77 (81.84) | |
| TNM-N | | | 0.035* | | 0.036* |
| N0 | 43 | 15(34.88) | | 116.05 (73.97) | |
| N1-N2 | 32 | 19 (59.38) | | 146.88 (70.82) | |
| TNM stage | | | 0.027* | | 0.012* |
| I-II | 62 | 24 (38.71) | | 119.19 (67.78) | |
| III-IV | 13 | 10 (76.92) | | 176.92 (84.99) | |
| Discovery time (years) | | | 0.202 | | 0.205 |
| <1 | 60 | 25 (41.67) | | 123.67 (73.44) | |
| ≥1 | 15 | 9(60.00) | | 151.33 (73.37) | |

Notes: *Significant difference. $^a\chi^2$ test is used for positive rate. $^b$Mann–Whitney test is used for staining score.
**Abbreviations**: SD, Standard deviation; TNM, Tumor-node-metastasis.

IgG expression and 5-year overall survival (OS) of the 75 breast cancer patients was elevated by the Kaplan–Meier method. The percent OS in SIA-IgG high expression (staining score ≥ 150) patients was significantly higher than that in SIA-IgG low expression (staining score < 150) patients ($P < 0.05$) (Figure 1h). Moreover, according to Cox multivariate analysis, the expression of SIA-IgG (hazard ratio = 1.822, $P = 0.040$) was an independent risk factor for poor prognosis in breast cancer patients (Table 2).

## Anti-SIA-IgG treatment could effectively suppress breast cancer cell growth, metastasis and invasion in vitro

In our past research, we demonstrated that SIA-IgG high breast cancer cells displayed high migration, metastasis and CSC-like characteristics, and knockdown of IgG reduced the proliferation, self-renewal, migration and invasion of MDA-MB-231, a claudin-low breast cancer cell-line, which was described for their properties of CSCs, but MCF-7 (a luminal-like breast cancer cell-line, which was described for their limited abilities to proliferate and migrate) there is no significant biological characteristics between SIA-IgG$^{high}$ group and

lSIA-IgG$^{low}$ group, indicating us SIA-IgG may play a more important role in the survival of breast cancer cells with high malignancy or with CSC-characteristics. To further explore whether SIA-IgG could be a potential therapeutic target for breast cancer, we blocked the function of SIA-IgG expressed by MDA-MB-231 cells utilizing the specific antibody RP215, and the same experiment was performed in MCF-7 and MCF-10A as controls. To dissect the change in breast cancer cell growth ability after blocking the functions of SIA-IgG, cell proliferation assays and colony formation assays were carried out. As shown in Figure 2(a,b) SIA-IgG-blocked MDA-MB-231 cells showed significant declines in the colony formation potential and proliferative rate, meanwhile there's no significant difference in MCF-7 as well as MCF-10 A. Moreover, after blocking the function of SIA-IgG, the apoptosis of MDA-MB-231 cells was only slightly increased without statistical significance (Figure 2c). Meanwhile, wound healing assay, Transwell migration and Matrigel invasion assays demonstrated that the migratory and invasive abilities of MDA-MB-231 cells were suppressed significantly when the function of SIA-IgG was blocked compared with the untreated cells (Figure 3(a–c)). These results revealed that

Table 2. Cox proportional hazards model analysis of prognostic factors in patients with breast cancer.

| Characteristics | HR | 95% CI | P value |
|---|---|---|---|
| Age (<50/≥50 years) | 1.881 | 1.039–3.405 | 0.037 |
| Pathological classification (ILC/IDC) | 2.310 | 0.864–6.178 | 0.095 |
| Pathological grade (I-II/III-IV) | 1.291 | 0.631–2.640 | 0.484 |
| Local invasion (T1-T2/T3-T4) | 1.950 | 0.957–3.974 | 0.066 |
| Lymph node metastasis (N0/N1-N2) | 2.436 | 1.302–4.559 | 0.005 |
| TNM stage (I-II/III-IV) | 1.391 | 0.605–3.197 | 0.437 |
| Tumor size (<5/≥5 cm$^3$) | 0.770 | 0.378–1.567 | 0.470 |
| RP215 staining (Low/High expression) [a] | 1.822 | 1.027–3.235 | 0.040 |

Notes: [a]SIA-IgG high expression, staining score ≥ 150. SIA-IgG low expression, staining score < 150.

**Abbreviations**: CI: confidence interval; HR: hazard ratio; TNM: tumor-node-metastasis.

targeting SIA-IgG could inhibit the proliferation, motility and invasion of MDA-MB-231 cells *in vitro*.

To verify the specificity of the antibody RP215, we have done a rescue experiment. We purified SIA-IgG from ascites of ovarian cancer by utilizing Protein G-affinity chromatography and RP215-affinity chromatography39. After adding SIA-IgG (5ug/ml) into the cell culture medium of MDA-MB-231 cell which were blocked by RP215 (2 μg/ml), the ability of cell proliferation and migration had been rescued (Figure 4).

## Anti-SIA-IgG treatment could effectively suppress breast cancer cell growth in vivo

To assess the effects of SIA-IgG treatment on tumor growth in vivo, we established xenograft tumor models using MDA-MB-231 cells and targeting SIA-IgG with its monoclonal antibody. All nude mice developed xenograft tumors at the injection site, and peritumoral injection of monoclonal antibody RP215 was performed (5 μg antibody per tumor, twice). The xenograft tumors were harvested at Day 9 after the first injection. Consistent with the in vitro results, in vivo experiments showed that MDA-MB-231 cells exhibited a significantly reduced growth rate in mice, as the tumor weight and average tumor volume in the RP215 antibody group (anti-SIA-IgG) were dramatically lower than those of the control group (mouse IgG), as shown in Figure 5(a–e). In addition, another xenograft model with MDA-MB-231 cells transfected with siRNA against IgG in nude mice further confirmed that targeting SIA-IgG could inhibit tumor growth in vivo (Figure 5 (f–h)). Collectively, our data indicated that anti-SIA-IgG treatment could effectively suppress SIA-IgG *in vitro* and *in vivo*.

## SIA-IgG may regulate biological features of breast cancer cells through Wnt/β-catenin pathway via mediate GSK3β

It has been proved that *Wnt*/β-catenin signaling pathway regulates cancer stem cell activity, promoting tumor progression and distant metastasis in breast cancer. In our previous study, the analyze data of RNA sequencing indicated SIA-IgG regulate biological characteristics of MDA-MB-231 cells may through *Wnt* signaling pathway (data not shown). At the present study, for further confirm this, we detected key molecular of *Wnt*/β-catenin signaling pathway after the expression of IgG was knocked down in MDA-MB-231 cells by western blotting. The results have shown that when SIA-IgG were knocked down, phosphorylates GSK3β at Ser9, which inhibits GSK3β activity, was also be inhibited, and knocking down of SIA-IgG also decreased total β-catenin level (Figure 6). These results indicate that SIA-IgG may through *Wnt*/β-catenin pathway via mediate GSK3β to regulate biological features of breast cancer cells, and Graphical Abstract presents the schematic of the possible acting site of SIA-IgG on *Wnt*/β-catenin pathway.

## Discussion

In our previous study, by using the monoclonal antibody RP215, we found abnormal sialic acid IgG (SIA-IgG) derived from non-B cells, and the results suggested that this type of SIA-IgG might be a potential treatment target for CSCs in breast cancer, and could be an indicator for its poor prognosis. [40] In this research, we have performed further studies to confirm these.

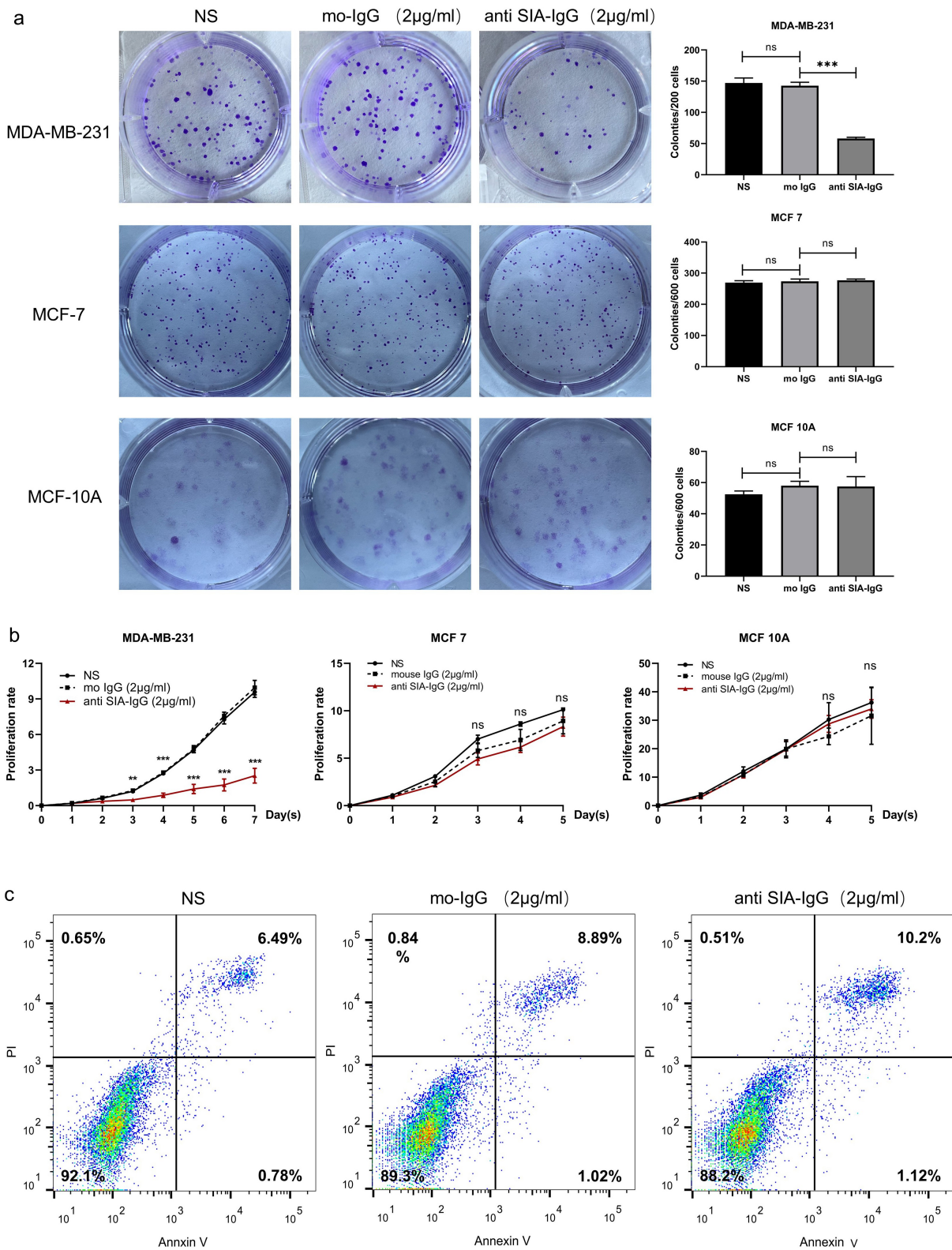First, we carried out clinical follow-up jobs and obtained 75 cases of breast cancer with overall

**Figure 2. Anti-SIA-IgG treatment effectively suppressed cell growth in MDA-MB-231**, MCF-7 and MCF-10A **cells**. (a) and (b), proliferation of SIA-IgG-treated MDA-MB-231, MCF-7 and MCF-10A cells were detected by clone formation assay and CCK-8 assay. (c) an apoptosis assay based on AV/PI flow cytometry was performed after the cells were treated with RP215 antibody, control antibody (mouse IgG) and saline for 48 h. Data are expressed as the means ± SEM. */#/a $P < 0.05$, **/##/aa $P < 0.01$, ***/###/aaa $P < 0.001$, and ns $P > 0.05$.
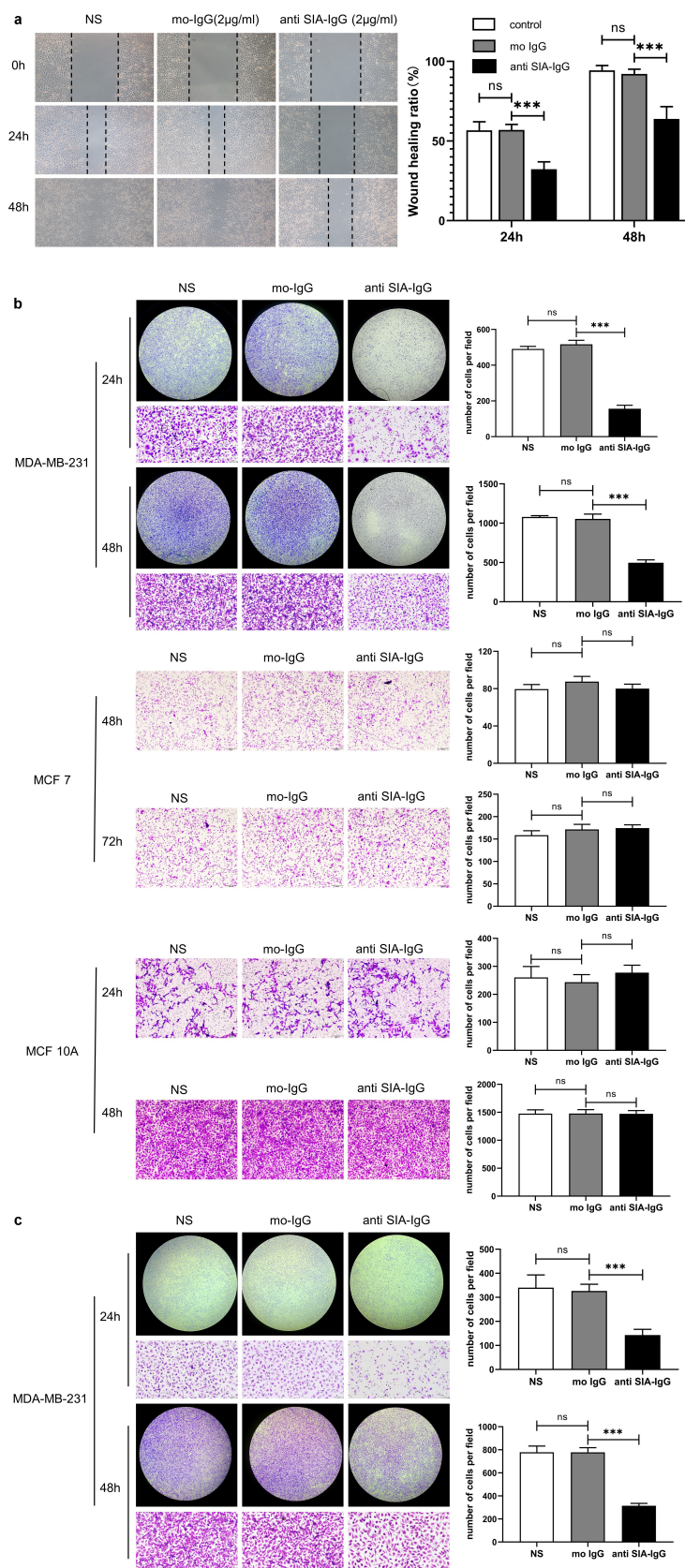
**Figure 3. Anti-SIA-IgG treatment effectively suppressed metastasis and invasion in MDA-MB-231 cells**. (a) the migration ability of MDA-MB-231 cells was analyzed by wound healing. Images were taken at 0, 24, and 48 h after antibody treatment. (b) and (c) the migration ability of MDA-MB-231, MCF-7 and MCF-10A cells were analyzed by Transwell assay. Images of MDA-MB-231 and MCF-10A cells were taken at 24 h and 48 h. Images of MCF-7 cells were taken at 48 h and 72 h. Invasion capacity of MDA-MB-231 were analyzed by and Transwell inserts coated with Matrigel matrix. Images were taken at 24 h and 48 h. The final concentrations of RP215 and control antibody used in the clone formation assay, apoptosis assay, wound healing assay, Transwell migration and invasion assays were 2 μg/ml. Data are expressed as the means ± SEM. * $P < 0.05$, ** $P < 0.01$, *** $P < 0.001$ and ns $P > 0.05$.
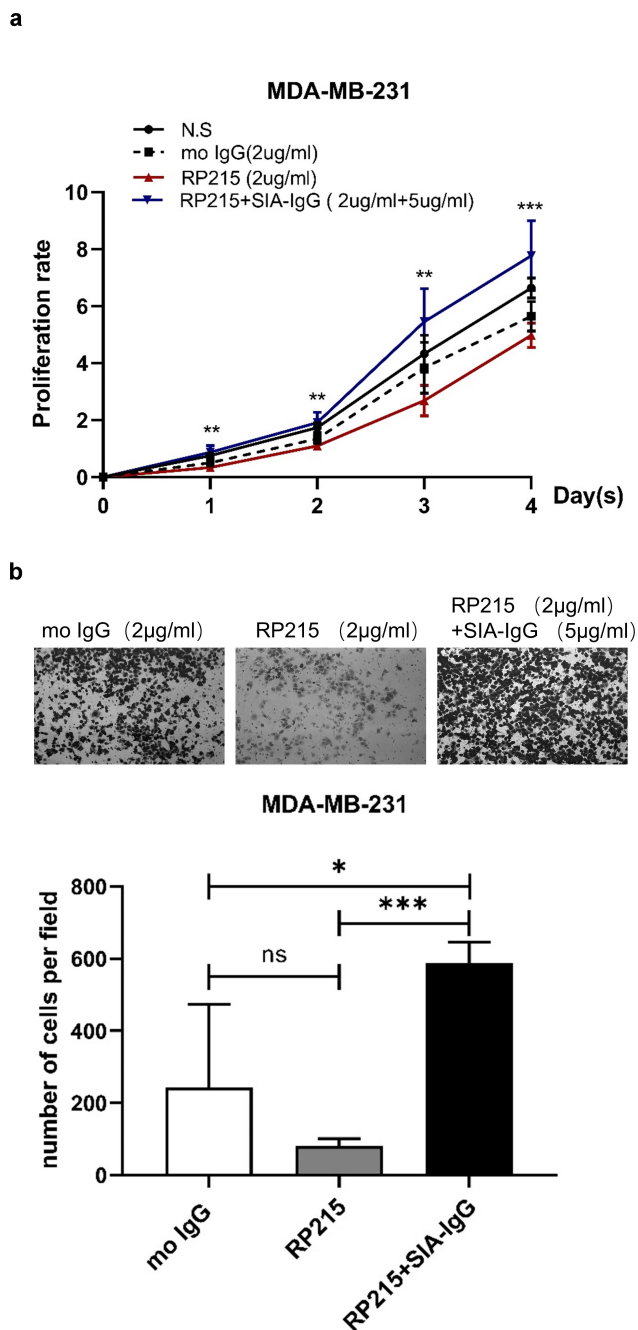
**a**



**b**



**Figure 4. Addition of SIA-IgG to MDA-MB-231 cells is able to rescue proliferation and migration**. (a–b), Functional rescue experiments were carried out in MDA-MB-231 cells including CCK-8 assay (Figure 4a) and transwell metastasis assay (Figure 4b). Data are expressed as the means ± SEM. * $P < 0.05$, ** $P < 0.01$, *** $P < 0.001$ and ns $P > 0.05$.

survival (OS), and all results showed that SIA-IgG could be an independent marker for poor prognosis of breast cancer. As the cases in the study was limited, we didn't categorize these cases by pathological classification. In our previously study, the SIA-IgG was highly expressed in in

cancer stem/progenitor-like cells, indicating that it might be a more sensitive and a more reliable poor prognosis indicator for some subtypes of breast cancer, such as triple negative breast cancer. This needs more focused and nuanced work in future.

Second, in order to verify whether SIA-IgG could be a antibody therapeutic target for breast cancer therapy, we blocked the function of SIA-IgG expressed by MDA-MB-231 cells by utilizing the monoclonal antibody RP215, and then explored the changes in their biological characteristics. The results shown that anti-SIA-IgG treatment could effectively suppress breast cancer cell growth, metastasis and invasion, and more research could be done to evaluate the effect of anti-SIA-IgG treatment work in combination with chemotherapeutics.

Moreover, in order to explore the possible mechanism, we detected key molecules of the $Wnt/\beta$-catenin signaling pathway after the expression of IgG was knocked down in MDA-MB-231 cells, and the results indicated that SIA-IgG may mediate GSK3β to regulate the biological features of breast cancer cells through the $Wnt/\beta$-catenin pathway. This study has not manipulated the express of GSK3β to verify this possibility, and further studies are needed to elucidate the mechanism in our future work.

There is one unexpected result in this work. When we have performed the rescue experiment, we found the cells from rescue group (with SIA-IgG and RP215) have stronger ability of proliferation and migration compared with the cells from control group (with mouse IgG or saline). The most likely explanation about this may be that we add more SIA-IgG than the rescue experiment needed.

There are also two shortcomings in this study. One is *in vivo*, we didn't perform toxicological analysis. And due to the limited conditions, we neither observe the aggregation and concentration of antibodies in tumors by label the antibodies with isotopes, nor observe the metastasis of tumors by PET-CT. Another shortcoming is the MCF-7 is a luminal-like breast cancer cell-line, which was described for their limited abilities to proliferate and migrate,
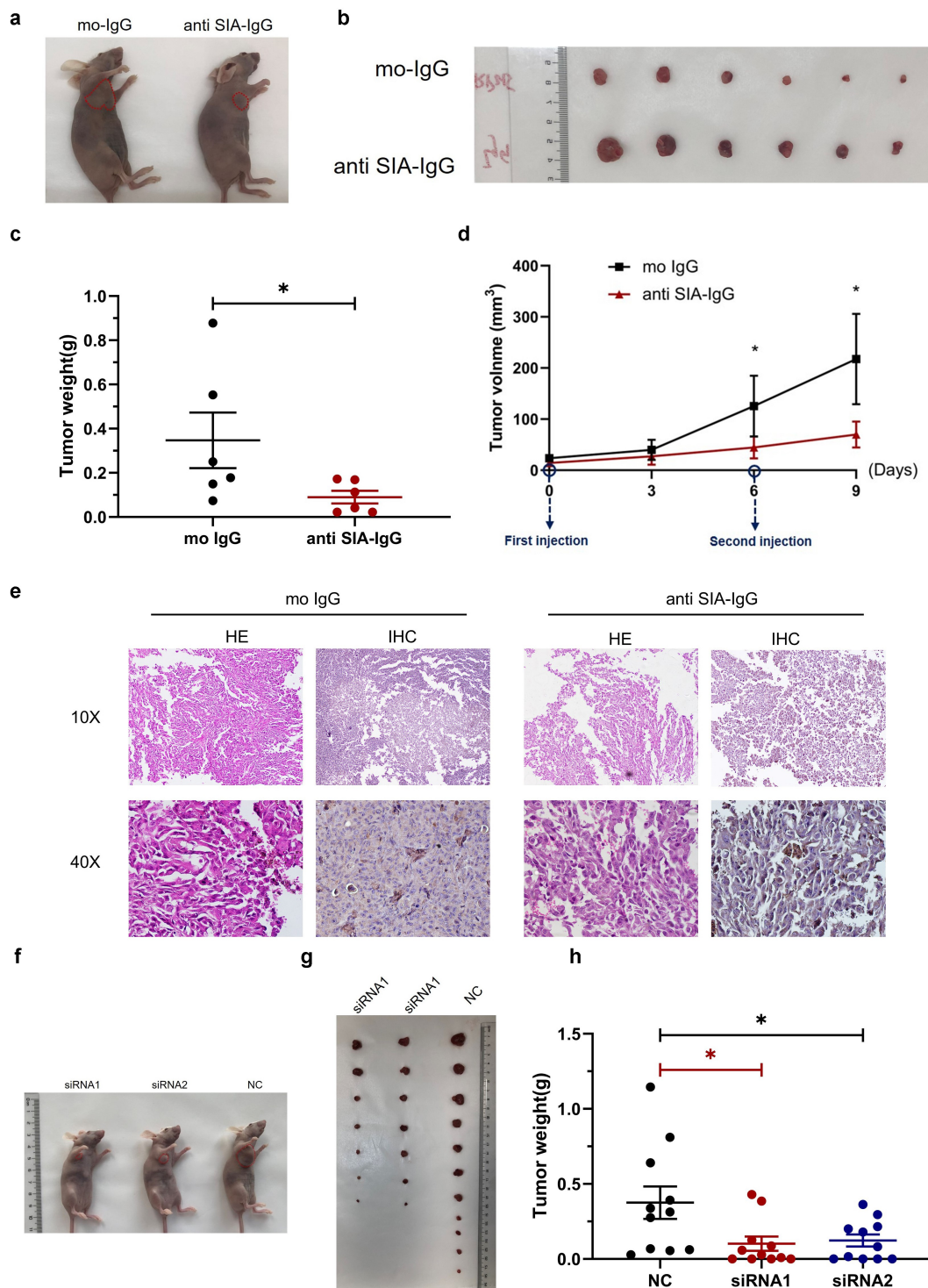
**Figure 5. Anti-SIA-IgG treatment effectively suppressed breast cancer cell growth in vivo**. (a–e), xenograft model in nude mice. Eight-week-old female nude mice were subcutaneously injected with $2 \times 10^6$ MDA-MB-231 cells, tumor nodules were harvested at Day 30 (Figure 3(a,b)), and tumor weights were measured (Figure 3c). During this period, peritumoral injection of monoclonal antibody RP215 and control antibody (mouse IgG) was performed separately at 5 μg per tumor twice. The length and width of tumors were measured every 3 days after the first subcutaneous injection, and tumor volume was calculated according to the formula $0.52 \times length \times width^2$ (Figure 3d). Tumor tissues from nude mice were then used for hematoxylin-eosin (HE) staining. In addition, we performed IHC staining to analyze SIA-IgG expression in tumor tissues from nude mice (Figure 3e). (f–h) three groups of 8-week-old female nude mice were subcutaneously injected with $2 \times 10^6$ MDA-MB-231 cells transfected with 2 siRNAs against IgG and control siRNA separately (group siRNA1, group siRNA2, group NC). The animals were sacrificed at Day 32, and the tumors were harvested (Figure 3(e,f)) and weighed (Figure 3g). Each Data are expressed as means ± SEM. * $P < 0.05$.
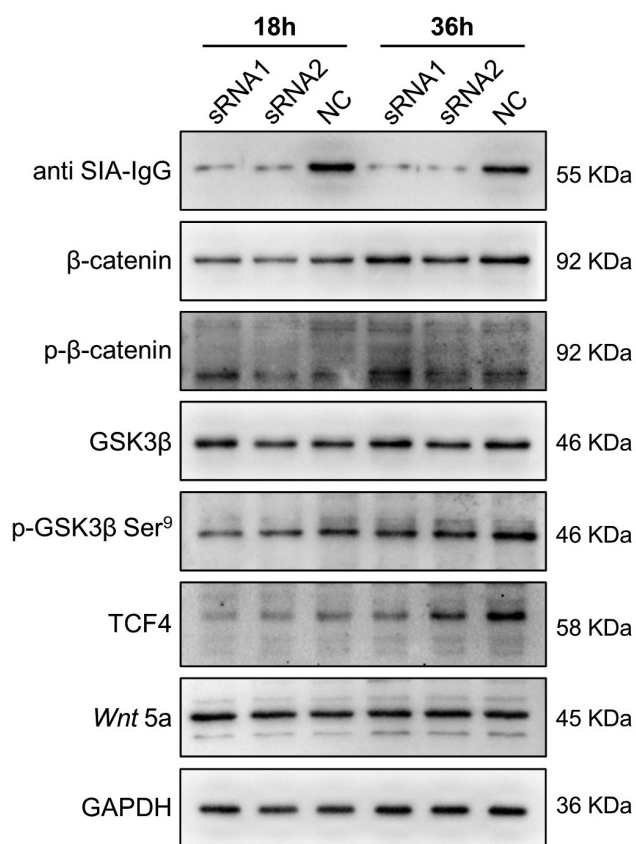
**Figure 6. SIA-IgG may regulate biological features of breast cancer cells through *Wnt*/β-catenin pathway via mediate GSK3β**. Detection of *Wnt*/β-catenin pathway related proteins by western blotting analysis in protein extracted from MDA-MB-231 cells which knocked IgG by siRNAs.

so the effect of SIA-IgG didn't be observed in this cell line.

Antibodies are wildly used in clinic. In the past two decades, the continuous discovery of multiple tumor related proteins and tumor stem cell markers has led to the emergence of multiple candidate targets for tumor therapy, which provides a lot of opportunities for the research and development of therapeutic antibodies. However, it is not that easy to develop therapeutic antibody. Firstly, the antibody must be a monoclonal antibody with high affinity and high specificity. Meanwhile, the target molecule of the antibody must be closely related to the occurrence and development of tumor. In addition, it would be better that the target molecule be located on cell membrane, ensure the therapeutic antibody can inhibit cell growth and even induce apoptosis by binding to the corresponding target. To sum up, RP215 is such a potential antibody molecule, demonstrating good anti-tumor effect in our research. The most important clinical implication of this study is providing a novel antibody therapeutic target in breast cancer, in particular for Triple negative breast cancer.

## Conclusion

This study showed that SIA-IgG could be an independent marker for poor prognosis of breast cancer by compared SIA-IgG expression, clinico-pathological characteristics and poor prognosis in 75 breast cancer cases. In addition, the results also presented SIA-IgG could be a therapeutic target for breast cancer therapy. What's more, the results indicated that SIA-IgG regulates the biological characteristics of MDA-MB-231 cells through the *Wnt* signaling pathway. Further studies are needed to elucidate the mechanism in our future work. Tumor immunotherapy holds great promise in breast cancer therapy, especially in the treatment for triple-negative breast cancer. This work provides new insights into the development of antibody therapeutic drug for breast cancer.

## Author contributions

Qinyuan Liao designed the experiments. Qinyuan Liao, Man Zhang, Jinhua Zheng and Junying Guo prepared the clinical samples and carried out all experiments. Man Zhang and Junying Guo carried out clinical follow-up jobs. Qinyuan Liao and Junying Guo carried out statistical analyses, Qiujin Zhang, Juan Du, Xiangfeng Zhao and Zhihua Wang were assisted in the experiments. Qinyuan Liao and Man Zhang wrote this article.

## Disclosure statement

No potential conflict of interest was reported by the author(s).

## Funding

## ORCID

Qinyuan Liao ⓘ http://orcid.org/0000-0002-2469-9675

## References

[1] Dong Y, Liao H, Yu J, et al. Incorporation of drug efflux inhibitor and chemotherapeutic agent into an inorganic/organic platform for the effective treatment of multidrug resistant breast cancer. J Nanobiotechnology. 2019;17(1):125.

[2] Zhang Y, Zhao CK, Li XL, et al. Virtual touch tissue imaging and quantification: value in malignancy prediction for complex cystic and solid breast lesions. Sci Rep. 2017;7(1):7807.

[3] Yao Y, Li X, Cheng L, et al. Circular RNA FAT atypical cadherin 1 (circFAT1)/microRNA-525-5p/spindle and kinetochore-associated complex subunit 1 (SKA1) axis regulates oxaliplatin resistance in breast cancer by activating the notch and Wnt signaling pathway. Bioengineered. 2021;12(1):4032–4043.

[4] Hennigs A, Riedel F, Gondos A, et al. Prognosis of breast cancer molecular subtypes in routine clinical care: a large prospective cohort study. BMC Cancer. 2016;16(1):1–9.

[5] Abu-Thuraia A, Goyette MA, Boulais J, et al. AXL confers cell migration and invasion by hijacking a PEAK1-regulated focal adhesion protein network. Nat Commun. 2020;11(1):3586.

[6] Xiu B, Chi Y, Liu L, et al. LINC02273 drives breast cancer metastasis by epigenetically increasing AGR2 transcription. Mol Cancer. 2019;18(1):187.

[7] Liu R, Shi P, Nie Z, et al. Mifepristone suppresses basal triple-negative breast cancer stem cells by down-regulating KLF5 expression. Theranostics. 2016;6(4):533–544.

[8] Gupta PB, Onder TT, Jiang G, et al. Identification of selective inhibitors of cancer stem cells by high-throughput screening. Cell. 2009;138(4):645–659.

[9] Tong M, Deng Z, Yang M, et al. Transcriptomic but not genomic variability confers phenotype of breast cancer stem cells. Cancer Commun (Lond). 2018;38(1):56.

[10] Jegatheeswaran S, Asnani A, Forman A, et al. Recognition of dimeric Lewis X by Anti-Dimeric Le(x) antibody SH2. Vaccines (Basel). 2020;8(3). DOI:10.3390/vaccines8030538.

[11] Haudek KC, Patterson RJ, Wang JL. SR proteins and galectins: what's in a name? Glycobiology. 2010;20 (10):1199–1207.

[12] Wang M, Zhu J, Lubman DM, et al. Aberrant glycosylation and cancer biomarker discovery: a promising and thorny journey. Clin Chem Lab Med. 2019;57(4):407–416.

[13] Cheng WK, Oon CE. How glycosylation aids tumor angiogenesis: an updated review. Biomed Pharmacother. 2018;103:1246–1252.

[14] Banerjee A, Lang JY, Hung MC, et al. Unfolded protein response is required in nu/nu mice microvasculature for treating breast tumor with tunicamycin. J Biol Chem. 2011;286(33):29127–29138.

[15] Kolbl AC, Andergassen U, Jeschke U. The role of glycosylation in breast cancer metastasis and cancer control. Front Oncol. 2015;5:219.

[16] Kamaruzman NI, Aziz NA, Poh CL, et al. Oncogenic signaling in tumorigenesis and applications of siRNA nanotherapeutics in breast cancer. Cancers (Basel). 2019;11(5):632.

[17] Babbage G, Ottensmeier CH, Blaydes J, et al. Immunoglobulin heavy chain locus events and expression of activation-induced cytidine deaminase in epithelial breast cancer cell lines. Cancer Res. 2006;66 (8):3996–4000.

[18] Huang J, Sun X, Mao Y, et al. Expression of immunoglobulin gene with classical V-(D)-J rearrangement in mouse brain neurons. Int J Biochem Cell Biol. 2008;40 (8):1604–1615.

[19] Chen Z, Gu J. Immunoglobulin G expression in carcinomas and cancer cell lines. FASEB J. 2007;21 (11):2931–2938.

[20] Zhu X, Wu L, Zhang L, et al. Distinct regulatory mechanism of immunoglobulin gene transcription in epithelial cancer cells. Cell Mol Immunol. 2010;7 (4):279–286.

[21] Niu N, Zhang J, Sun Y, et al. Expression and distribution of immunoglobulin G and its receptors in an immune privileged site: the eye. Cell Mol Life Sci. 2011;68(14):2481–2492.

[22] Niu N, Zhang J, Guo Y, et al. Expression and distribution of immunoglobulin G and its receptors in the human nervous system. Int J Biochem Cell Biol. 2011;43(4):556–563.

[23] Qiu X, Sun X, He Z, et al. Immunoglobulin gamma heavy chain gene with somatic hypermutation is frequently expressed in acute myeloid leukemia. Leukemia. 2013;27(1):92–99.

[24] Zheng J, Huang J, Mao Y, et al. Immunoglobulin gene transcripts have distinct VHDJH recombination characteristics in human epithelial cancer cells. J Biol Chem. 2009;284(20):13610–13619.

[25] Zhang S, Mao Y, Huang J, et al. Immunoglobulin gene locus events in epithelial cells of lactating mouse mammary glands. Cell Mol Life Sci. 2010;67(6):985–994.

[26] Huang J, Sun X, Gong X, et al. Rearrangement and expression of the immunoglobulin mu-chain gene in human myeloid cells. Cell Mol Immunol. 2014;11 (1):94–104.

[27] Hu F, Zhang L, Zheng J, et al. Spontaneous production of immunoglobulin M in human epithelial cancer cells. PLoS One. 2012;7(12):e51423.

[28] Liang PY, Li HY, Zhou ZY, et al. Overexpression of immunoglobulin G prompts cell proliferation and inhibits cell apoptosis in human urothelial carcinoma. Tumour Biol. 2013;34(3):1783–1791.

[29] Deng H, Ma J, Jing Z, et al. Expression of immunoglobulin A in human mesangial cells and its effects on cell apoptosis and adhesion. Mol Med Rep. 2018;17 (4):5272–5282.

[30] Jiang D, Ge J, Liao Q, et al. IgG and IgA with potential microbial-binding activity are expressed by normal human skin epidermal cells. Int J Mol Sci. 2015;16 (2):2574–2590.

[31] Qiu X, Zhu X, Zhang L, et al. Human epithelial cancers secrete immunoglobulin g with unidentified specificity to promote growth and survival of tumor cells. Cancer Research. 2003;63(19):6488.

[32] Chen Z, Huang X, Ye J, et al. Immunoglobulin G is present in a wide variety of soft tissue tumors and correlates well with proliferation markers and tumor grades. Cancer. 2010;116(8):1953–1963.

[33] Li X, Ni R, Chen J, et al. The presence of IGHG1 in human pancreatic carcinomas is associated with immune evasion mechanisms. Pancreas. 2011;40 (5):753–761.

[34] Yang B, Ma C, Chen Z, et al. Correlation of immunoglobulin G expression and histological subtype and stage in breast cancer. PLoS One. 2013;8(3): e58706.

[35] Zhang L, Hu S, Korteweg C, et al. Expression of immunoglobulin G in esophageal squamous cell carcinomas and its association with tumor grade and Ki67. Hum Pathol. 2012;43(3):423–434.

[36] Lee G, Ge B. Cancer cell expressions of immunoglobulin heavy chains with unique carbohydrate-associated biomarker. Cancer Biomark. 2009;5(4):177–188.

[37] Lee G, Laflamme E, Chien CH, et al. Molecular identity of a pan cancer marker, CA215. Cancer Biol Ther. 2008;7(12):2007–2014.

[38] Lee G. Cancer cell-expressed immunoglobulins: CA215 as a pan cancer marker and its diagnostic applications. Cancer Biomark. 2009;5(3):137–142.

[39] Tang J, Zhang J, Liu Y, et al. Lung squamous cell carcinoma cells express non-canonically glycosylated IgG that activates integrin-FAK signaling. Cancer Lett. 2018;430:148–159.

[40] Liao Q, Liu W, Liu Y, et al. Aberrant high expression of immunoglobulin G in epithelial stem/progenitor-like cells contributes to tumor initiation and metastasis. Oncotarget. 2015;6(37):40081–40094.

[41] Liu Y, Liu D, Wang C, et al. Binding of the monoclonal antibody RP215 to immunoglobulin G in metastatic lung adenocarcinomas is correlated with poor prognosis. Histopathology. 2015;67(5):645–653.

[42] Qin C, Sheng Z, Huang X, et al. Cancer-driven IgG promotes the development of prostate cancer though the SOX2-CIgG pathway. Prostate. 2020;80 (13):1134–1144.

[43] Cui M, You L, Zheng B, et al. High expression of cancer-derived glycosylated immunoglobulin G predicts poor prognosis in pancreatic ductal adenocarcinoma. J Cancer. 2020;11(8):2213–2221.

[44] Sheng Z, Liu Y, Qin C, et al. IgG is involved in the migration and invasion of clear cell renal cell carcinoma. J Clin Pathol. 2016;69(6):497–504.

[45] Sheng Z, Liu Y, Qin C, et al. Involvement of cancer-derived IgG in the proliferation, migration and invasion of bladder cancer cells. Oncology Letters. 2016;12(6):5113–5121.

[46] Lee G, Cheung AP, Ge B, et al. CA215 and GnRH receptor as targets for cancer therapy. Cancer Immunol Immunother. 2012;61(10):1805–1817.

[47] Lee G, Chu RA, Ting HH. Preclinical assessment of anti-cancer drugs by using RP215 monoclonal antibody. Cancer Biol Ther. 2009;8(2):161–166.

[48] Zhang G, Xu Z, Yu M, et al. Bcl-2 interacting protein 3 (BNIP3) promotes tumor growth in breast cancer under hypoxic conditions through an autophagy-dependent pathway. Bioengineered. 2022;13(3):6280–6292.

[49] Xueqin T, Jinhong M, Yuping H. Inhibin subunit beta A promotes cell proliferation and metastasis of breast cancer through Wnt/beta-catenin signaling pathway. Bioengineered. 2021;12(2):11567–11575.

[50] Zhuang W, Niu T, Li Z. MicroRNA miR-145-5p regulates cell proliferation and cell migration in colon cancer by inhibiting chemokine (C-X-C motif) ligand 1 and integrin alpha2. Bioengineered. 2021;12 (2):9909–9917.

[51] Liang S, Zhang X, Li J. Zinc finger Asp-His-His-Cys palmitoyl -acyltransferase 19 accelerates tumor progression through wnt/beta-catenin pathway and is upregulated by miR-940 in osteosarcoma. Bioengineered. 2022;13(3):7367–7379.

[52] Zhang J, Shang L, Jiang W, et al. Shikonin induces apoptosis and autophagy via downregulation of pyrroline-5-carboxylate reductase1 in hepatocellular carcinoma cells. Bioengineered. 2022;13 (3):7904–7918.

[53] Han B, Ge Y, Cui J, et al. Down-regulation of lncRNA DNAJC3-AS1 inhibits colon cancer via regulating miR-214-3p/LIVIN axis. Bioengineered. 2020;11 (1):524–535.

[54] Li C, Jin W, Zhang D, et al. Clinical significance of microRNA-1180-3p for colorectal cancer and effect of

its alteration on cell function. Bioengineered. 2021;12 (2):10491–10500.

[55] Toyoda H, Kumada T, Tada T, et al. Differences in the impact of prognostic factors for hepatocellular carcinoma over time. Cancer Science. 2017;108 (12):2438–2444.